Neuropilin-2–Mediated Tumor Growth and Angiogenesis in Pancreatic Adenocarcinoma

Nikolaos A. Dallas,[1] Michael J. Gray,[1] Ling Xia,[2] Fan Fan,[2] George van Buren II,[1] Puja Gaur,[1] Shaija Samuel,[2] Sherry J. Lim,[1] Thiruvengadam Arumugam,[2] Vijaya Ramachandran,[2] Huamin Wang,[3] and Lee M. Ellis[1,2]

Abstract

Purpose. Neuropilin-2 (NRP-2) is a coreceptor for vascular endothelial growth factor (VEGF) on endothelial cells. NRP-2 is overexpressed in pancreatic ductal adenocarcinoma (PDAC) cells relative to nonmalignant ductal epithelium. This study determined the role of NRP-2 in PDAC cells.

Experimental Design. NRP-2 expression was reduced in PDAC cells with stable short-hairpin RNA (shRNA) transfection. Western blotting was done to evaluate signaling intermediates. Migration and invasion studies were carried out in Boyden chambers. Anchorage-independent growth was assessed by soft-agar colony formation. *In vivo* growth was evaluated using murine subcutaneous and orthotopic xenograft models. Immunohistochemical analysis evaluated *in vivo* proliferation and angiogenesis.

Results. shRNA-NRP-2 decreased NRP-2 levels without affecting neuropilin-1 levels. Akt activation was decreased in clones with reduced NRP-2 (shRNA-NRP-2). shRNA-NRP-2 cells showed decreased migration, invasion, and anchorage-independent growth compared with control cells. *In vitro* proliferation rates were similar in control- and shRNA-transfected cells. Subcutaneous and orthotopic xenografts from shRNA-transfected cells were significantly smaller than those resulting from control-transfected cells ($P < 0.05$). Furthermore, shRNA-NRP-2 tumors exhibited less cellular proliferation and decreased microvascular area relative to control tumors ($P < 0.05$). Constitutive expression of the angiogenic mediator Jagged-1 was reduced in shRNA-NRP-2 cells, whereas vascular endothelial growth factor levels were unchanged.

Conclusion. Reduction of NRP-2 expression in PDAC cells decreased survival signaling, migration, invasion, and ability to grow under anchorage-independent conditions. *In vivo*, reduction of NRP-2 led to decreased growth of xenograft tumors and decreased vascular area, which was associated with decreased Jagged-1 levels. NRP-2 is a potential therapeutic target on PDAC cells.

In 2008, there will be an estimated 37,680 new cases of pancreatic ductal adenocarcinoma (PDAC) in the United States (1). PDAC is associated with a dismal prognosis, with a 5-year survival rate of only 3% to 4% independent of stage (2). For more than a decade, the deoxycytidine analogue gemcitabine was the only U.S. Food and Drug Administration-approved chemotherapeutic agent used for PDAC based on its alleviation of disease-related symptoms and its modest survival advantage over 5-fluorouracil (3). More recently, the addition of targeted therapeutics to gemcitabine regimens has been thoroughly evaluated in phase III clinical trials. In one trial that compared gemcitabine and gemcitabine plus erlotinib, the epidermal growth factor receptor tyrosine kinase inhibitor, the combination therapy provided a small but statistically significant improvement in survival, which led to eventual Food and Drug Administration approval (4). In a similarly designed trial, the addition of cetuximab, the monoclonal antibody to epidermal growth factor receptor, to a gemcitabine regimen did not improve the efficacy of gemcitabine. Despite promising results in a phase II trial, the addition of bevacizumab, the anti-vascular endothelial growth factor (VEGF) monoclonal antibody, to a gemcitabine regimen did not provide any benefit over gemcitabine alone (5). Given the dismal prognosis for patients with PDAC and the lack of significant improvement in overall survival with the current mainstays of targeted therapy, a better understanding of tumor growth, with the goal of identification of novel targets for therapy, is imperative.

Although bevacizumab, when combined with gemcitabine, did not improve the effects of gemcitabine in a phase III clinical trial, recent preclinical evidence suggests that other VEGF-associated molecules may be valid targets for therapy in patients with PDAC (6–8). The VEGF family of ligands and receptors is involved in many physiologic and pathologic processes (9). In humans, there are five known VEGF family ligands (VEGF-A, VEGF-B, VEGF-C, VEGF-D, and placental

Authors' Affiliations: Departments of [1]Surgical Oncology, [2]Cancer Biology, and [3]Pathology, The University of Texas M. D. Anderson Cancer Center, Houston, Texas
Received 6/13/08; revised 8/18/08; accepted 8/22/08.

Grant support: NIH grants T32 CA09599 (N.A. Dallas, P. Gaur, G. van Buren, and S.J. Lim) and grants R01 CA112390 (L.M. Ellis), R.E. "Bob" Smith Fund for Cancer Research (S. Samuel), William C. Liedtke, Jr., Fund for Cancer Research (L.M. Ellis), and NIH Cancer Center Support Grant CA016672.

The costs of publication of this article were defrayed in part by the payment of page charges. This article must therefore be hereby marked *advertisement* in accordance with 18 U.S.C. Section 1734 solely to indicate this fact.

Requests for reprints: Lee M. Ellis, Department of Surgical Oncology, The University of Texas M. D. Anderson Cancer Center, Unit 444, P.O. Box 301402, Houston, TX 77230-1402. Phone: 713-792-6926; Fax: 713-792-4689; E-mail: lellis@mdanderson.org.

doi:10.1158/1078-0432.CCR-08-1520

Translational Relevance

Pancreatic cancer remains a disease with a mortality rate of >95% due to the fact that effective therapy is lacking. To develop more effective therapies, it is essential to identify potential targets in preclinical models that can lead to the development of new agents to counter this disease. NRP-2 is a protein that, in addition to its known role on endothelial cells, mediates processes directly involved in tumor growth and thus may serve as a novel target for therapy.

growth factor) and three structurally related tyrosine kinase receptors [VEGF receptor (VEGFR)-1, VEGFR-2, and VEGFR-3; reviewed in ref. 10]. Coreceptors for the VEGFRs include neuropilin-1 and neuropilin-2 (NRP-2), which were first identified based on their role in axonal guidance and neuronal development (11–14).

Neuropilin-1 and NRP-2 are 130- to 140-kDa nontyrosine kinase transmembrane glycoproteins with unique protein structures that share 44% sequence homology (15). Although expression of the neuropilins was originally thought to be limited to neurons, these receptors have since been identified on inflammatory cells (16), vascular smooth muscle cells (17), endothelial cells (13, 18), and, most recently, tumor cells (reviewed in ref. 10). Given their lack of an intracellular kinase domain, it was originally thought that the downstream effects of neuropilins were dependent on their association with other transmembrane receptors and their ability to increase the binding affinity of the ligands to these receptors, thereby increasing downstream signaling. However, recent data suggest that neuropilins can signal via their short intracellular domain directly by recruiting neuropilin-interacting protein or synectin to the cell membrane (19–21).

NRP expression on tumor cells is correlated with a more malignant phenotype in melanoma (22) and in breast (23, 24), prostate (25), colorectal (26–28), and pancreatic (8, 28) cancers. Recently, our laboratory showed that NRP-2 in colorectal cancer regulates tumor growth, and exploration of small interfering RNA therapies identified this molecule as a potential therapeutic target in this disease (26). Using an antibody targeting murine NRP-2, others showed that inhibition of NRP-2 in a preclinical lung metastasis model prevented tumor metastases by blocking the formation of tumor-associated lymphatics (29). We and others have shown that PDAC specimens exhibit greater expression of NRP-2 than nonmalignant ductal epithelium does (6). Given these findings, we sought to identify the role of NRP-2 in PDAC. Through a series of experiments, we studied the effects of reducing NRP-2 on PDAC cells both *in vitro* and in xenograft models.

Materials and Methods

Human tissue specimens and cell lines. Formalin-fixed, paraffin-embedded primary PDAC specimens and adjacent nonmalignant pancreatic tissue were obtained from an established tumor bank at The University of Texas M. D. Anderson Cancer Center following protocols approved by the institutional review board.

The human PDAC cell lines AsPC-1, BxPC3, MiaPaCa2, MPanc96, and Panc-1 were obtained from the American Type Culture Collection. L3.6pl cells were kindly provided by I.J. Fidler D.V.M., PhD. (The University of Texas M. D. Anderson Cancer Center). All cells were cultured and maintained at 37°C with 5% CO_2 in MEM supplemented with 10% fetal bovine serum (FBS), 2 units/mL penicillin-streptomycin mixture (Flow Laboratories), vitamins (Life Technologies), 1 mmol/L sodium pyruvate, 2 mmol/L L-glutamine, and nonessential amino acids. *In vitro* experiments were done at 60% to 80% cell confluence and at early passages after receipt from their supplier.

Generation of NRP-2 short-hairpin RNA cell lines. Short-hairpin RNA (shRNA) expression vectors targeting NRP-2 were created as described previously (26). Briefly, two NRP-2 targeting sequences were identified, and oligonucleotides encoding each sequence followed by a 9-bp hairpin sequence were generated. The targeting sequences were as follows: 5′-CCCAACCAGAAGATTGTCC-3′ for NP2#1 and 5′-GTCAG-CACTAATGGAGAGG-3′ for NP2#2. The oligonucleotides were then ligated into the pSilencer 4.0 shRNA expression system (Ambion) at compatible sites, generating the shRNA expression plasmids, shNP2Vec#1 and shNP2Vec#2. Negative-control shRNA expression plasmids, shConVec#1 and shConVec#2, were generated in a similar fashion by scrambling the NRP-2 targeting sequences and verifying through NIH Basic Local Alignment Search Tool analysis that the scrambled sequences were not substantially homologous with any vertebrate genes.

The stable NRP-2 knockdown cell lines, shNRP2-C21 and shNRP2-C23, were created by transfecting BxPC3 cells with 0.5 ng of each shNP2Vec plasmid using FuGENE 6 transfection reagent (Roche Diagnostics) according to the manufacturer's protocols. The stable control-transfected cell line, shCon, was generated similarly using both scramble sequence-encoding shNRP expression plasmids. Selected clones were isolated and maintained in medium containing 50 μg/mL hygromycin B (Roche Diagnostics). NRP-2 expression levels in all resulting cell lines were determined by Western blot analysis.

Western blotting. Cells were plated and grown to 70% to 80% confluence before protein extraction. Whole-cell lysates were obtained using radioimmunoprecipitation assay B protein lysis buffer as described previously (30). To isolate secreted proteins, cells were plated in 1% FBS-supplemented medium for 48 h, and conditioned medium was harvested and concentrated using Amicon Ultra Centrifugal Filter Devices (Millipore). Isolated proteins were quantitated using a modified Bradford assay (Bio-Rad Laboratories). Protein samples for Western blotting were prepared, boiled, and separated using SDS-PAGE on an 8% or 15% gel and transferred to a polyvinylidene difluoride membrane (Millipore) by electroblotting. Antibodies were diluted in TBS and 0.1% (v/v) Tween with 5% nonfat dry milk after 1 h protein blocking in the absence of antibody. Membranes were incubated at 4°C overnight and then washed and incubated with the appropriate horseradish peroxidase-conjugated secondary antibody (Amersham Biosciences) for 1 h at room temperature. Protein bands were visualized using a commercially available enhanced chemiluminescence kit (Amersham Biosciences). Antibodies used included neuropilin-1, NRP-2, and Jagged-1 (Santa Cruz Biotechnology); phospho-Akt^{Ser473}, Akt, phospho-extracellular signal-regulated kinase 1/2$^{Thr202/Tyr204}$, extracellular signal-regulated kinase 1/2, phospho-Src^{Tyr416}, and Src (Cell Signaling Technology); phospho-VEGFR-1^{Tyr1213} (Millipore); VEGFR-1 (Oncogene Research Products); and VEGF-A (R&D Systems). For verification of equal protein loading, all membranes were stripped and reprobed for either β-actin or vinculin (Sigma-Aldrich). When indicated, densitometric analysis was used to quantitate differences in protein levels from blots using NIH ImageJ v1.34 software.[4]

[4] http://rsb.info.nih.gov/ij

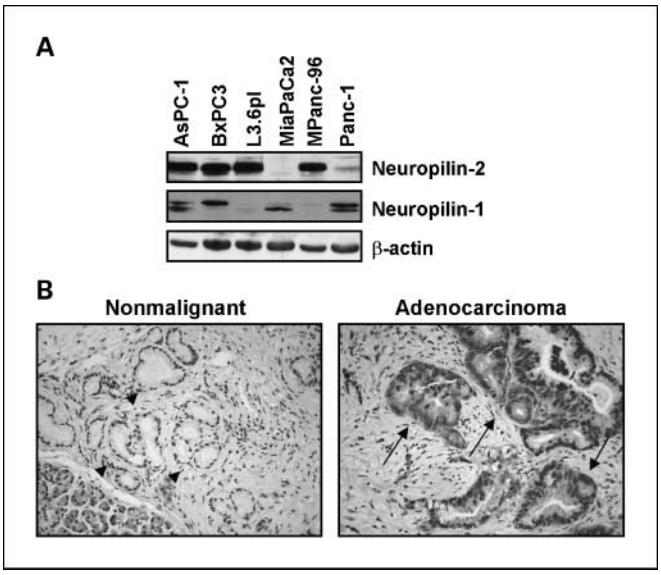

Fig. 1. Expression of NRP-2 in pancreatic adenocarcinoma. *A,* NRP-2 was expressed in 5 of the 6 pancreatic cell lines as determined by Western blotting. *B,* immunohistochemical staining of specimens from a nonmalignant pancreas and from pancreatic adenocarcinoma. NRP-2 was expressed in pancreatic adenocarcinoma cells (*arrows*) but not in normal ductal structures (*arrowheads*). Magnification, ×20.

Cell proliferation and chemosensitivity. *In vitro* cellular proliferation was determined using a 3-(4,5-dimethylthiazol-2-yl)-2,5-diphenyltetrazolium bromide assay as described previously (26). Briefly, 2,500 cells of each cell line (parental, shCon, shNRP2-C21, and shNRP2-C23) were plated in each well. At each time point (0, 24, 48, and 72 h), 40 μL 3-(4,5-dimethylthiazol-2-yl)-2,5-diphenyltetrazolium bromide solution was added to each well, and the plates were incubated for 1 h at 37°C. Colorimetric analysis after the addition of DMSO was done using a standard microplate reader.

Migration and invasion assays. Migration assays were done as described previously (7). Briefly, 75,000 control- or shNRP2-transfected cells were suspended in 500 μL of 1% FBS-supplemented medium and placed in an insert with 8 μm pores, which was lowered into 750 μL of 10% FBS-supplemented medium in a standard Boyden chamber assay. After 24 h incubation, migrated cells on the underside of the membrane were fixed and stained using the Protocol HEMA 3 stain set (Fisher Scientific). Membranes were excised, mounted, and examined under light microscopy at ×20 magnification. Migrated cells were counted in five random fields.

Invasion assays were done using a similar protocol with minor modifications. The inserts used in the invasion assays were coated with Matrigel (BD Biosciences) and prehydrated with 1% FBS-supplemented medium for 30 min before the addition of the cell suspension. Invasion chambers were incubated for 48 h, and the numbers of invading cells were again quantified.

Anchorage-independent growth assays. Soft-agar assays were used to determine the effect of reduced NRP-2 expression on the ability to grow in anchorage-independent conditions. Each well of a 6-well plate was coated with 1 mL of 10% FBS-supplemented medium with 1% agarose. After 20 min, cell suspensions containing control- and shNRP2-transfected cells (500 cells each) were added in 1 mL medium with 0.5% agarose. Cells were incubated for 14 days under standard conditions (37°C, 5% CO_2) with the addition of 300 μL medium every 3 days to hydrate the exposed agarose. At the end of the incubation period, wells were examined under a light microscope at ×20 magnification, and the number of colonies larger than 50 μm was counted per well.

Xenograft models. Male athymic nude mice, 6 to 8 weeks old, were obtained from the National Cancer Institute-Frederick Cancer Research Facility and acclimated for 2 weeks. All animal studies were conducted under approved guidelines of the Animal Care and Use Committee of The University of Texas M. D. Anderson Cancer Center. Equal numbers of cells (10^6) from the shCon, shNRP2-C21, and shNRP2-C23 cell lines were suspended in 100 μL PBS and injected subcutaneously into the right rear flank of each mouse (10 mice per group). Tumor growth was observed and recorded over 10 weeks. When tumors in the control group exceeded 1.5 cm in longest diameter, mice were killed by CO_2 asphyxiation according to protocol, and tumors were excised. Tumors were weighed and measured, and a portion of each was placed in either 10% formalin (for paraffin embedding) or OCT compound or was snap-frozen in liquid nitrogen. Tumor volume was calculated as $0.5 \times (\text{width}^2) \times (\text{length})$.

The results of the subcutaneous xenograft study were validated with an orthotopic pancreatic tumor model. BxPC3-shCon and shNRP2 cells were infected with a luciferase-reporter gene using a recombinant

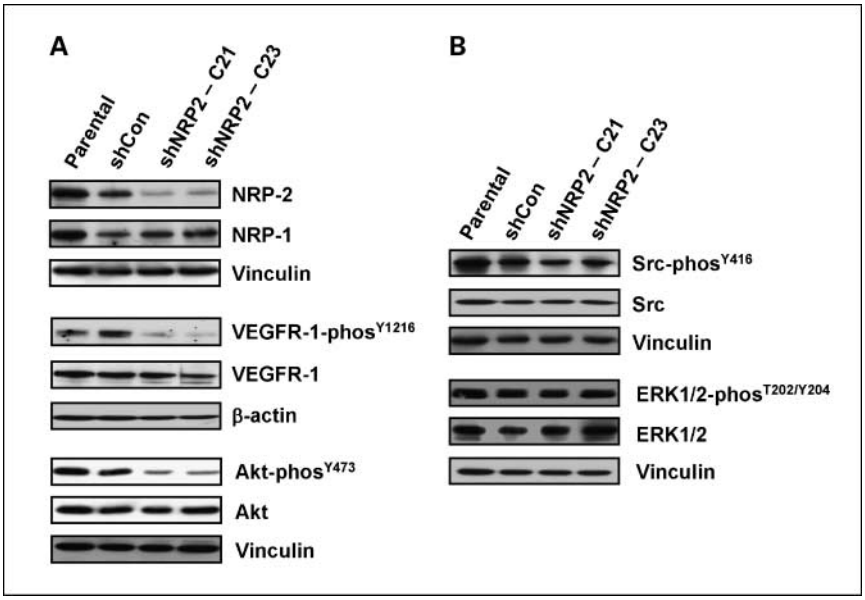

Fig. 2. Effect of shRNA to NRP-2 on intracellular signaling in BxPC3 cells. *A,* Western blots showing specific knockdown of NRP-2 in the BxPC3 human pancreatic cancer cell line by plasmid-mediated stable transfection using shRNA to NRP-2. shCon cells were transfected with a scrambled sequence. VEGFR-1 and Akt phosphorylation was reduced in cells with reduced NRP-2 expression. Vinculin and β-actin levels served as loading controls. *B,* Src phosphorylation was moderately reduced in shNRP2 clones relative to that in control-transfected cells. Levels of phosphorylated and total extracellular signal-regulated kinase 1/2 were unchanged.

lentivirus as described previously (31). In each of 10 mice, a suspension of 2×10^6 luciferase-labeled shCon or shNRP2 cells in 50 μL PBS was injected into the tail of the pancreas through a left-flank incision under ketamine/xylazine (Sigma-Aldrich) anesthesia. Mice were killed at 50 days when 2 to 3 mice in any group showed signs of lethargy. Tumors were weighed, measured, and processed as in the subcutaneous model.

Immunohistochemical and immunofluorescence analysis. Tumors preserved in formalin were placed in paraffin blocks and sectioned onto positively charged microscope slides. They were deparaffinized in xylene, hydrated in graded alcohol, and pretreated for antigen retrieval in citrate buffer for 20 min in a 98°C steamer. Tumor sections embedded in OCT compound were sectioned onto positively charged microscopy slides and serially immersed in acetone, a 1:1 (v/v) acetone/chloroform mixture, and then acetone. Slides were then stained with H&E to assess morphology, with proliferating cell nuclear antigen to visualize proliferative nuclei, with terminal deoxynucleotidyl transferase-mediated biotin-dUTP nick end labeling to visualize apoptotic cells, or with CD31 to visualize blood vessels. All immunohistochemical sections were counterstained with Gill no. 3 hematoxylin (Sigma-Aldrich).

Antibodies and materials used included rat anti-mouse CD31 (Pharmingen), mouse anti-human proliferating cell nuclear antigen PC-10 (DAKO), and the DeadEnd Fluorometric Terminal Deoxynucleotidyl Transferase-Mediated Biotin-dUTP Nick End Labeling System (Promega). Immunofluorescence slides were examined using a Nikon Microphot FXA fluorescence microscope, and representative images were obtained.

To determine the digitized microvascular area (D-MVA), CD31 fluorescently stained slides were analyzed using NIH ImageJ v1.34 software. The red channel, corresponding to CD31 staining, was isolated and digitized into a binary image, with black indicating stained vessels and white indicating no staining. Vessels with lumens were digitally filled, and a composite D-MVA was quantitated.

In vivo *bioluminescence imaging*. Bioluminescence imaging of luciferase-expressing cells in the orthotopic tumor model was done using the IVIS 100 imaging system coupled to a data acquisition personal computer equipped with Living Image software (Xenogen). Tumor cell-inoculated mice were anesthetized with a 1.5% isoflurane-oxygen mixture and injected intraperitoneally with luciferase potassium salt solution (Sigma-Aldrich) at a dose of 150 mg/kg body weight immediately before imaging. *In vivo* images were obtained on days 3, 18, 39, and 50, and photon emission representative of luciferase activity was used assess relative tumor burden in the mice.

Results

Expression of NRP-2 in human pancreatic adenocarcinoma. Western blot analysis of 6 commonly used pancreatic cancer cell lines showed that 5 of 6 expressed NRP-2 to varying degrees (Fig. 1A). When tissue from PDAC surgical specimens was analyzed for NRP-2 expression, NRP-2 was detected in 7 of 11 (64%) adenocarcinomas but not in any of 4 specimens of adjacent nonmalignant tissue; representative images are shown

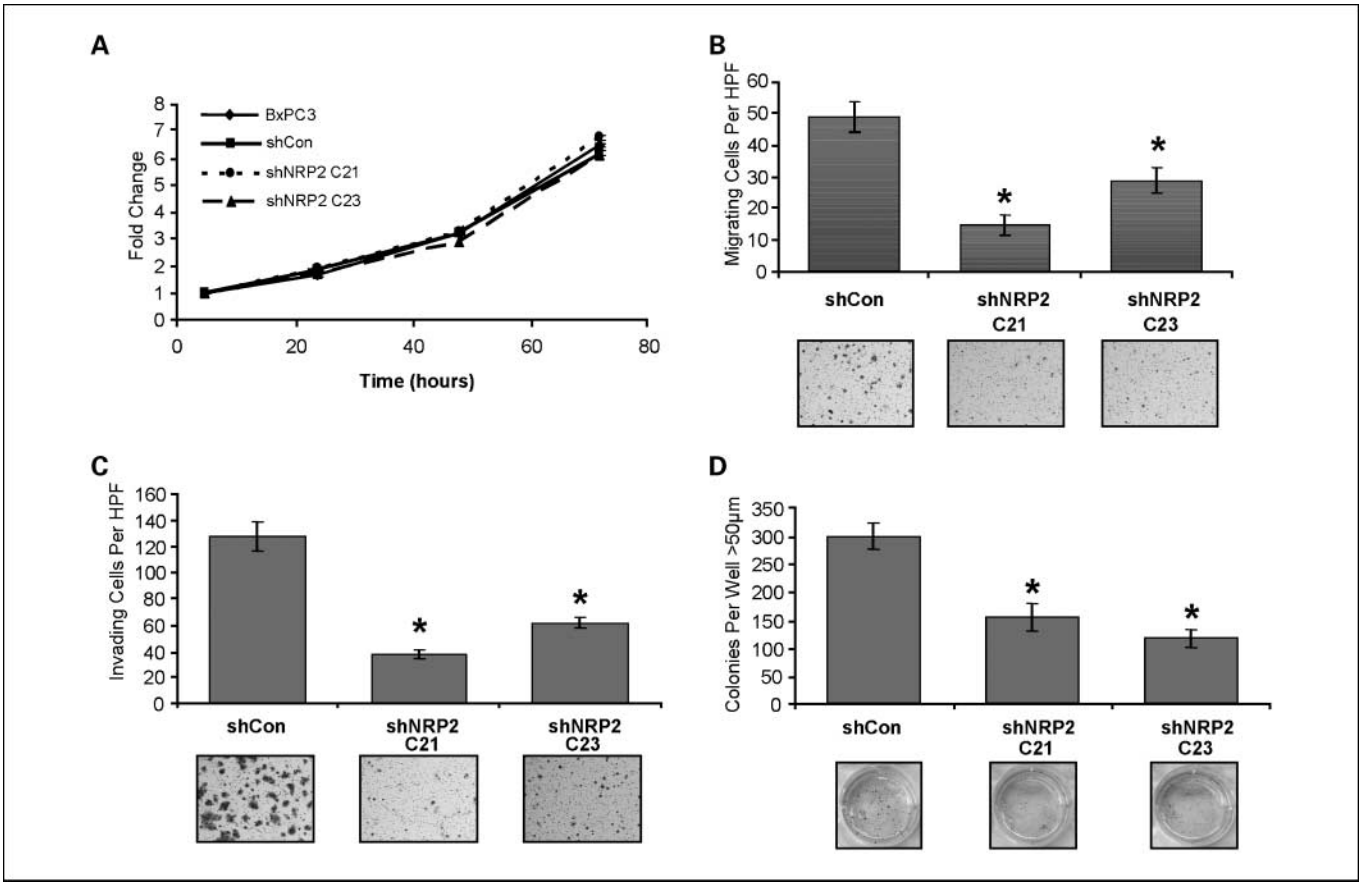

Fig. 3. Effect of reduced NRP-2 on the *in vitro* phenotype of pancreatic cancer cells. *A,* control-transfected cells and shNRP2 cells had similar proliferation rates. *B* and *C,* cells with reduced NRP-2 were less migratory in Boyden chamber assays (*B*) and less invasive across a biologic barrier (*C*) than scramble control-transfected cells. *D,* reduction of NRP-2 led to decreased growth in soft agar. *Bars,* SE. *, $P < 0.05$. *HPF,* high-power microscopic field.

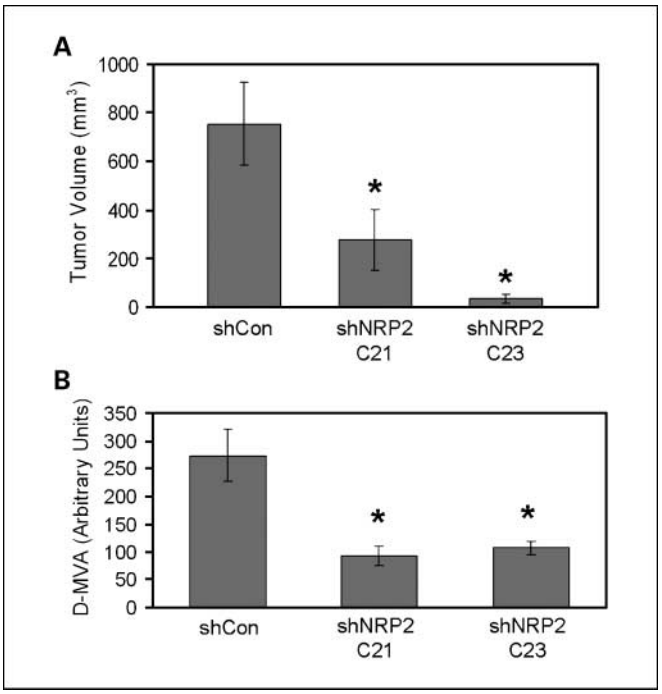

Fig. 4. Effect of reduced NRP-2 expression on tumor growth and *in vivo* proliferation. *A,* tumors derived from shNRP2 cells were significantly smaller than shCon-derived tumors. *B,* quantification of D-MVA of shCon and shNRP2 tumor sections revealed that shNRP2-derived tumors had 61% to 66% smaller D-MVA than that in control tumors ($P < 0.05$). *Bars,* SE. *, $P < 0.05$.

in Fig. 1B. In specimens designated positive, all visualized tumor cells stained positively for NRP-2 expression.

Reduced NRP-2 expression alters constitutive signaling in pancreatic cancer cells. shRNA-NRP-2 decreased NRP-2 without any effect on neuropilin-1. Because the neuropilins are coreceptors for VEGFRs in both tumor cells and endothelial cells, we determined the effect of reduced NRP-2 expression on constitutive activation of VEGFR-1 in BxPC3 cells. This cell line expresses VEGFR-1 but not VEGFR-2 or VEGFR-3 (by reverse transcription-PCR analysis; data not shown). The reduction of NRP-2 expression was associated with a decrease in phosphorylation of VEGFR-1 in these cells relative to control-transfected cells (Fig. 2A). Furthermore, survival signaling, as measured by Western blotting for phospho-Akt, was reduced in cells transfected with shRNA to NRP-2. This finding was confirmed in transfected MPanc96 cells (data not shown). Other intracellular signaling molecules were evaluated to investigate the role of NRP-2 in cellular signaling. We determined that Src phosphorylation was also moderately reduced in shNRP-2 cells, but extracellular signal-regulated kinase 1/2 levels were unchanged relative to those in control-transfected cells (Fig. 2B).

Reduced NRP-2 expression decreases migration, invasion, and anchorage-independent growth. A 3-(4,5-dimethylthiazol-2-yl)-2,5-diphenyltetrazolium bromide assay was used to determine the effect of reduced NRP-2 expression on *in vitro* proliferation rates. The shCon and shNRP2 clones showed similar *in vitro* proliferation rates up to 72 h after plating (Fig. 3A).

To evaluate the effect of reduced NRP-2 expression on *in vitro* migration and invasion, a standard Boyden chamber assay was used. Pancreatic cancer cells with shRNA to NRP-2 showed a 40% to 70% decrease in ability to migrate (Fig. 3B; $P < 0.05$) and a 50% to 70% decrease in ability to invade through a Matrigel-coated membrane (Fig. 3C; $P < 0.05$).

The ability of cells to survive and replicate under anchorage-independent conditions was evaluated using a soft-agar growth assay. Cells with reduced NRP-2 produced significantly fewer clones in soft agar than did control-transfected cells ($P < 0.05$).

Reduced NRP-2 expression leads to decreased* in vivo *tumor growth and alters the tumor vasculature. Given the decrease in migratory and invasive behavior and the reduction in anchorage-independent growth of cells deficient in NRP-2, we next investigated the role of NRP-2 in *in vivo* growth. Growth characteristics were first evaluated using a murine subcutaneous xenograft model. After 10 weeks, mice inoculated with shNRP2-transfected cells grew tumors that were 63% to 95% smaller than those of mice inoculated with shCon-transfected cells (Figs. 4A and 5A-C; $P < 0.05$). Furthermore, despite similar *in vitro* proliferation rates, analysis of tumors by proliferating cell nuclear antigen staining showed a significant decrease in *in vivo* proliferation in the shNRP2 groups. Specifically, tumors derived from shNRP2-transfected cells had ~65% fewer proliferative nuclei per field relative to those in tumors from shCon-transfected cells ($P < 0.05$). No differences were seen in the numbers of apoptotic cells in the tumors by terminal deoxynucleotidyl transferase-mediated biotin-dUTP nick end labeling staining (data not shown).

A follow-up study was designed to validate our findings in an orthotopic model using shCon- and shNRP2-transfected cells labeled with firefly luciferase. Before mouse implantation, 2×10^5 cells were plated in 12-well plates, and equal luciferase activity in each cell line was verified *in vitro* (data not shown). Cells were then prepared and injected orthotopically into the tails of the mouse pancreases. As seen on bioluminescence imaging, tumors derived from shNRP2 cells grew more slowly than did the shCon-derived tumors (Fig. 6A and B; $P < 0.05$). At the time of tumor harvest, shNRP2 tumors were significantly smaller than shCon tumors; average tumor masses were 0.50 g for shCon tumors and 0.08 g for shNRP2 tumors (Fig. 6C; $P < 0.05$), corroborating the data from the subcutaneous model.

Reduced NRP-2 expression on tumor cells alters the tumor vasculature. Tumor morphologic characteristics were evaluated by standard H&E staining, which showed qualitative differences between groups (Fig. 5D-F). Although tumors derived from shCon-transfected cells formed contiguous tumor cell clusters with stromal elements, those from shNRP2-transfected cells contained patchy acellular areas suggestive of regions of restrained growth within the tumors. Given the decreased number of proliferative cells in the shNPR2-derived tumor sections (Fig. 5G-I), we hypothesized that the inhibition of growth may be due to a secondary effect via limited tumor angiogenesis. Immunohistochemical staining for CD31 was then used to evaluate the number and morphologic characteristics of blood vessels within each tumor. Vessels in shCon tumors were subjectively larger with more visible patent lumens (Fig. 5J-L). Vessels were enumerated by counting the number of discrete stained structures within each field without regard to vessel size or patency. There was no difference in absolute vessel number between groups. D-MVA was analyzed to incorporate vessel size and

patency into our analysis of the tumor vasculature by providing an estimate of integrated lumen area and presumably blood flow orthogonal to the tumor section. shNRP2 tumors had a 61% to 66% decrease in D-MVA than shCon tumors (Figs. 4B and 5M-O; $P < 0.05$).

Reduced NRP-2 expression is associated with decreased Jagged-1 levels. The reduction of D-MVA led us to hypothesize that the effects on development of the tumor vasculature may be due to altered angiogenic mediator expression in the tumor cells themselves. To investigate this hypothesis, we used Western blotting to identify differences in protein levels of several known angiogenic mediators. There were no differences in VEGF-A, VEGF-C, or delta-like ligand-4 levels between shCon- and shNRP2-transfected cells (data not shown); however, there was a significant reduction (46% in shNRP2-C21 and 53% in shNRP2-C23) in Jagged-1 levels in cells deficient in NRP-2 relative to that in control cells (Fig. 7A and B).

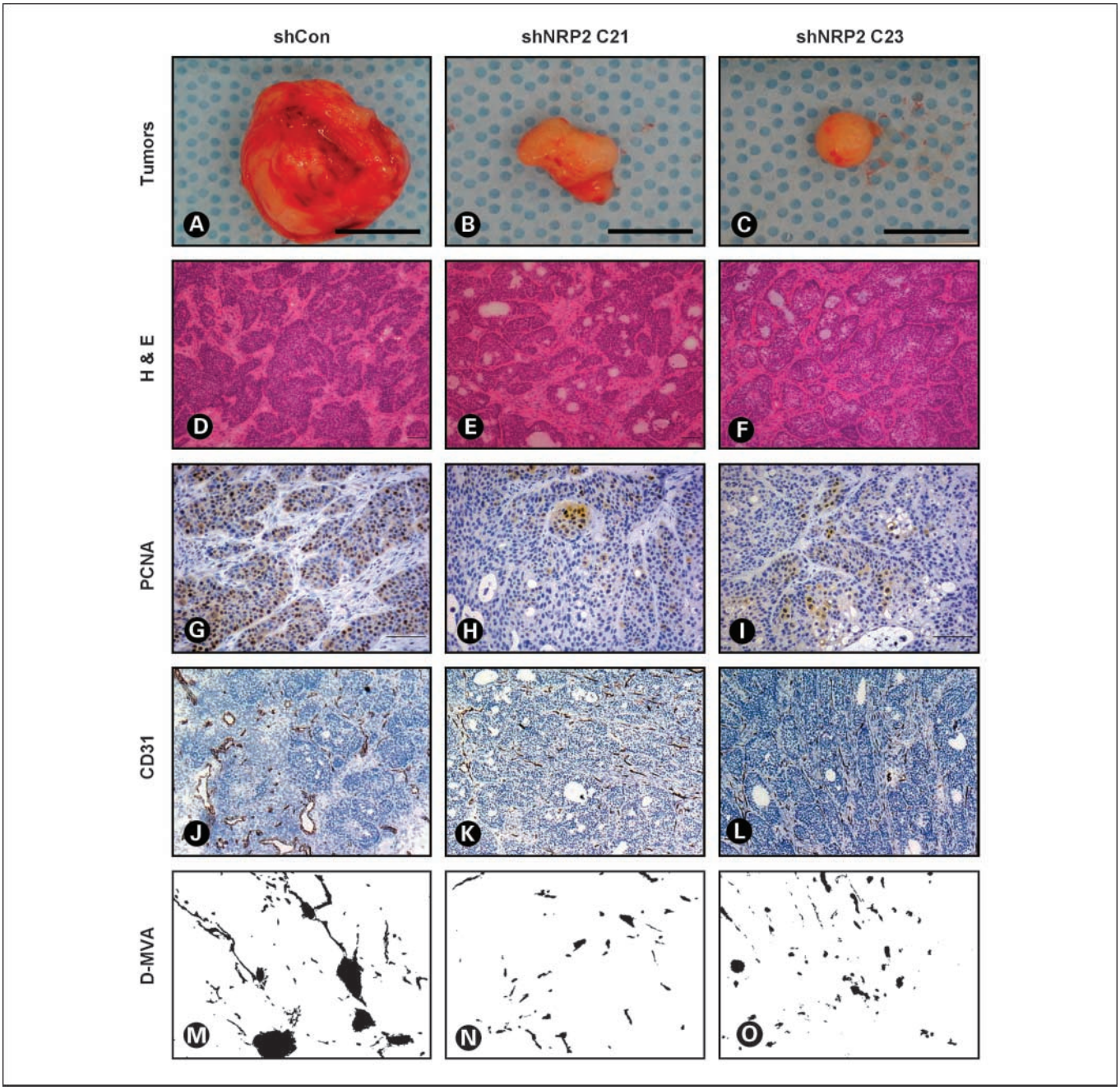

Fig. 5. Effect of reduced NRP-2 expression on tumor growth, *in vivo* proliferation, and tumor vasculature in a subcutaneous model. *A* to *C,* tumors derived from shNRP2 cells were significantly smaller than shCon-derived tumors. *D* to *F,* H&E staining of shNRP2 tumors showed more necrotic foci throughout the tumor than there were in shCon tumors. *G* to *I,* proliferating cell nuclear antigen staining showed significantly fewer proliferative cells in shNRP2 tumors than in shCon tumors. *J* to *L,* CD31 staining revealed more patent vessels per field in the shCon specimens. *M* to *O,* binary images of CD31 staining with lumens digitally filled show higher D-MVA in shCon tumor sections relative to those with reduced NRP-2 expression.

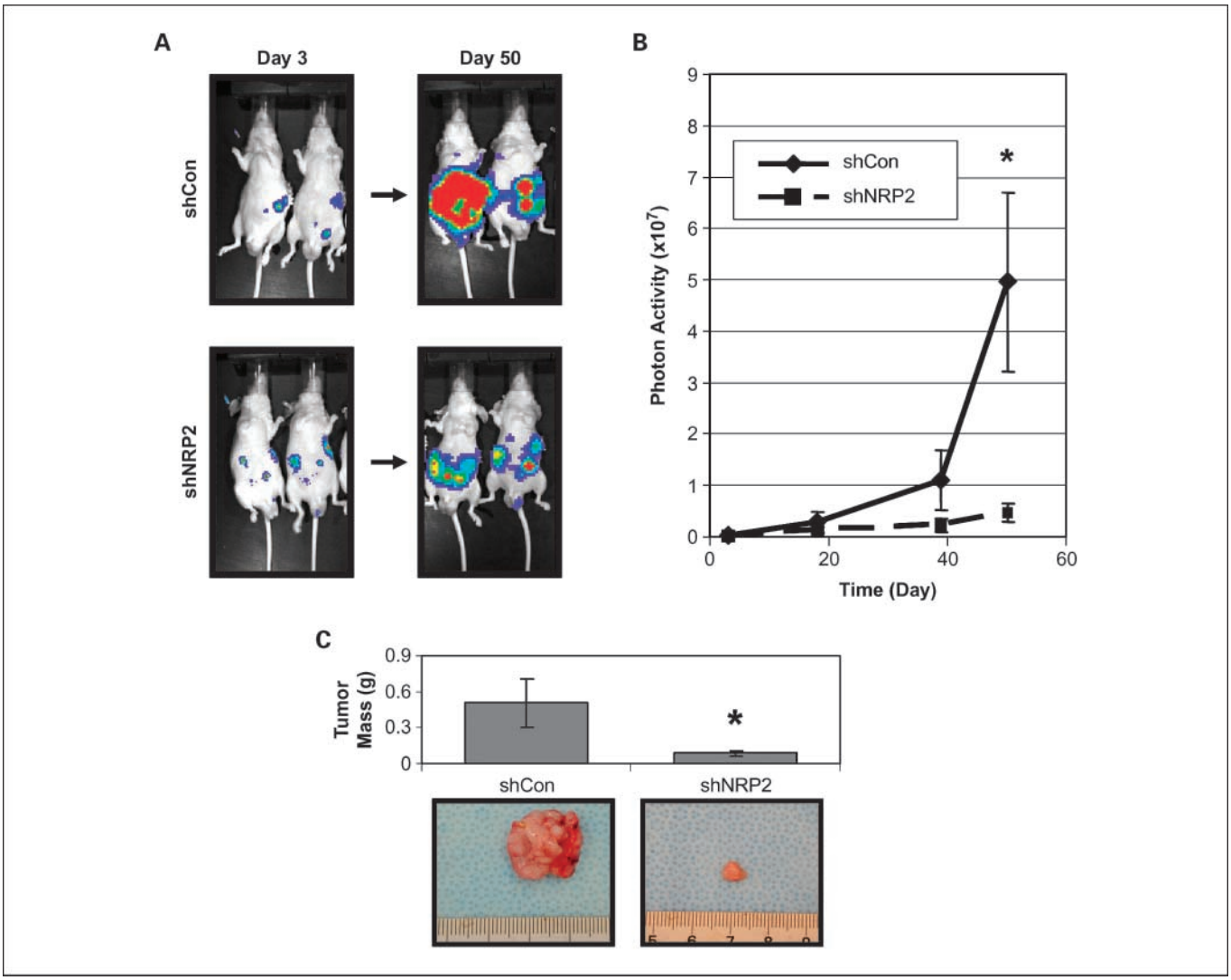

Fig. 6. Effect of reduced NRP-2 expression on orthotopic xenograft growth. Two million pancreatic cancer BxPC3 cells transfected with either a scrambled (shCon) or targeting sequence against NRP-2 (shNRP2) and labeled with firefly luciferase were injected orthotopically into the tail of each mouse pancreas, and tumors were allowed to grow for 50 d. Mice were injected with luciferin substrate and imaged four times during tumor growth. *A,* representative mice from each group at the first (day 3) and final (day 50) time points. *B,* photon activity was plotted against time for mice in each group. *C,* at the time of their harvest, tumors derived from shNRP2 cells were significantly smaller than those from shCon cells. *Bars,* SE. *, $P < 0.05$.

Discussion

PDAC is associated with poor outcome and a high mortality rate. Attempts to treat this malignancy with standard chemotherapeutics or, more recently, targeted agents have led to minimal improvements in disease-related measures or the overall mortality rate. New therapeutic strategies are essential if we are to improve the lives of patients with this disease.

Our results showed that NRP-2 is overexpressed in pancreatic cancer cell lines and human PDAC specimens relative to nonmalignant ductal epithelium. Reduced NRP-2 expression in cell lines led to decreased tumor growth, identifying NRP-2 as a potential therapeutic target in this malignancy. Although a decrease in NRP-2 expression had no effect on *in vitro* proliferation, tumors derived from NRP-2 knockdown pancreatic cancer cells had significantly fewer proliferative nuclei and a smaller functional blood vessel area in cross-sectional analysis. An orthotopic xenograft tumor model confirmed the findings of the subcutaneous model: NRP-2-deficient cells had significantly less *in vivo* tumor growth than control-transfected cells did.

Although the expression of NRP-2 in vascular and lymphatic endothelial cells has been described, few studies have investigated its role in tumor cells. Our group recently showed that NRP-2 in colorectal carcinoma plays a role in several critical aspects of the malignant phenotype (26). The results of this study confirm prior work done in our laboratory on PDAC and extend it by highlighting the importance of tumor-derived NRP-2 and its indirect effect on the tumor vasculature. We found that, similar to the case in colorectal cancer, NPR-2 in PDAC is involved in survival signaling, migration, invasion, and anchorage-independent growth *in vitro*. Furthermore, *in vivo*, we showed in two

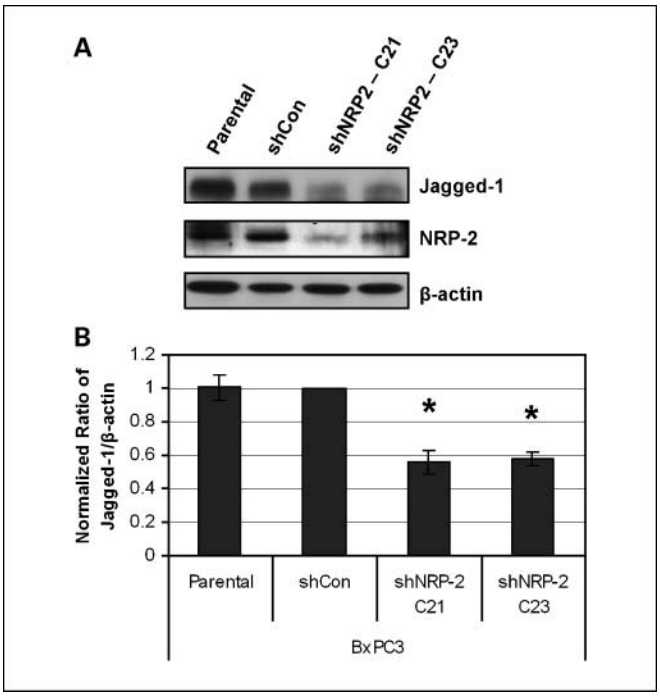

Fig. 7. Effect of reduced NRP-2 expression on Jagged-1 levels. *A,* Western blotting showed that stable reduction of NRP-2 by shRNA was associated with a decrease in Jagged-1 protein levels. *B,* densitometric analysis of three independent experiments confirmed that Jagged-1 protein levels were reduced by 46% to 53% in cells deficient in NRP-2. *Bars,* SE. *, $P < 0.05$ versus shCon.

independent experiments at two different sites that cells deficient in NRP-2 had decreased tumor growth. We showed that NRP-2-deficient cells *in vitro* had similar proliferation rates to those of control-transfected cells, suggesting that the reduction of tumor growth *in vivo* was not due to inherent proliferative capacity.

These data suggest that the reduction of tumor growth may have been due to the secondary effect on angiogenesis as shown by D-MVA quantitation and the decrease in functional vasculature within the tumor. The reduction in tumor vasculature with the loss of NRP-2 expression was associated with a decrease in Jagged-1 expression in the tumor cells. Jagged-1 is a member of the Notch family of ligands and receptors known to play a role in developmental angiogenesis and, more recently, tumor angiogenesis (reviewed in ref. 32). Others have shown that increased Jagged-1 expression in tumor cells leads to increased endothelial capillary network sprouting *in vitro* and angiogenesis *in vivo* (33). Our data showed that a decrease in Jagged-1 expression after experimental reduction of NRP-2 levels in tumor cells is associated with a lower D-MVA, although a causal relationship has not been established. In conclusion, our data provide evidence that NRP-2 on tumor cells may serve as a therapeutic target in PDAC.

Disclosure of Potential Conflicts of Interest

L.M. Ellis: commercial research grants, Sanofi-Aventis, honoraria, Genentech.

References

1. Jemal A, Siegel R, Ward E, et al. Cancer statistics, 2008. CA Cancer J Clin 2008;58:71–96.
2. Ko AH, Tempero MA. Treatment of metastatic pancreatic cancer. J Natl Compr Canc Netw 2005;3:627–36.
3. Burris HA III, Moore MJ, Andersen J, et al. Improvements in survival and clinical benefit with gemcitabine as first-line therapy for patients with advanced pancreas cancer: a randomized trial. J Clin Oncol 1997;15:2403–13.
4. Moore MJ, Goldstein D, Hamm J, et al. Erlotinib plus gemcitabine compared with gemcitabine alone in patients with advanced pancreatic cancer: a phase III trial of the National Cancer Institute of Canada Clinical Trials Group. J Clin Oncol 2007;25:1960–6.
5. Kindler HL, Niedzwiecki D, Hollis D, et al. A double-blind, placebo-controlled, randomized phase III trial of gemcitabine (G) plus bevacizumab (B) versus gemcitabine plus placebo (P) in patients (pts) with advanced pancreatic cancer (PC): a preliminary analysis of Cancer and Leukemia Group B (CALGB) 80303. In: ASCO Gastrointestinal Symposium; 2007 Jan 19-21; Orlando, FL. abstract 108.
6. Fukahi K, Fukasawa M, Neufeld G, Itakura J, Korc M. Aberrant expression of neuropilin-1 and -2 in human pancreatic cancer cells. Clin Cancer Res 2004;10:581–90.
7. Wey JS, Fan F, Gray MJ, et al. Vascular endothelial growth factor receptor-1 promotes migration and invasion in pancreatic carcinoma cell lines. Cancer 2005;104:427–38.
8. Wey JS, Gray MJ, Fan F, et al. Overexpression of neuropilin-1 promotes constitutive MAPK signalling and chemoresistance in pancreatic cancer cells. Br J Cancer 2005;93:233–41.
9. Ferrara N, Gerber HP, LeCouter J. The biology of VEGF and its receptors. Nat Med 2003;9:669–76.
10. Dallas NA, Fan F, Gray MJ, et al. Functional significance of vascular endothelial growth factor receptors on gastrointestinal cancer cells. Cancer Metastasis Rev 2007;26:433–41.
11. Kawakami A, Kitsukawa T, Takagi S, Fujisawa H. Developmentally regulated expression of a cell surface protein, neuropilin, in the mouse nervous system. J Neurobiol 1996;29:1–17.
12. Kolodkin AL, Levengood DV, Rowe EG, Tai YT, Giger RJ, Ginty DD. Neuropilin is a semaphorin III receptor. Cell 1997;90:753–62.
13. Soker S, Takashima S, Miao HQ, Neufeld G, Klagsbrun M. Neuropilin-1 is expressed by endothelial and tumor cells as an isoform-specific receptor for vascular endothelial growth factor. Cell 1998;92:735–45.
14. Gluzman-Poltorak Z, Cohen T, Herzog Y, Neufeld G. Neuropilin-2 is a receptor for the vascular endothelial growth factor (VEGF) forms VEGF-145 and VEGF-165 [corrected]. J Biol Chem 2000;275:18040–5.
15. Staton CA, Kumar I, Reed MW, Brown NJ. Neuropilins in physiological and pathological angiogenesis. J Pathol 2007;212:237–48.
16. de Paulis A, Prevete N, Fiorentino I, et al. Expression and functions of the vascular endothelial growth factors and their receptors in human basophils. J Immunol 2006;177:7322–31.
17. Stephenson JM, Banerjee S, Saxena NK, Cherian R, Banerjee SK. Neuropilin-1 is differentially expressed in myoepithelial cells and vascular smooth muscle cells in preneoplastic and neoplastic human breast: a possible marker for the progression of breast cancer. Int J Cancer 2002;101:409–14.
18. Soker S, Gollamudi-Payne S, Fidder H, Charmahelli H, Klagsbrun M. Inhibition of vascular endothelial growth factor (VEGF)-induced endothelial cell proliferation by a peptide corresponding to the exon 7-encoded domain of VEGF165. J Biol Chem 1997;272:31582–8.
19. Bielenberg DR, Klagsbrun M. Targeting endothelial and tumor cells with semaphorins. Cancer Metastasis Rev 2007;26:421–31.
20. Cai H, Reed RR. Cloning and characterization of neuropilin-1-interacting protein: a PSD-95/Dlg/ZO-1 domain-containing protein that interacts with the cytoplasmic domain of neuropilin-1. J Neurosci 1999;19:6519–27.
21. Gao Y, Li M, Chen W, Simons M. Synectin, syndecan-4 cytoplasmic domain binding PDZ protein, inhibits cell migration. J Cell Physiol 2000;184:373–9.
22. Straume O, Akslen LA. Increased expression of VEGF-receptors (FLT-1, KDR, NRP-1) and thrombospondin-1 is associated with glomeruloid microvascular proliferation, an aggressive angiogenic phenotype, in malignant melanoma. Angiogenesis 2003;6:295–301.
23. Timoshenko AV, Rastogi S, Lala PK. Migration-promoting role of VEGF-C and VEGF-C binding receptors in human breast cancer cells. Br J Cancer 2007;97:1090–8.
24. Starzec A, Vassy R, Martin A, et al. Antiangiogenic and antitumor activities of peptide inhibiting the vascular endothelial growth factor binding to neuropilin-1. Life Sci 2006;79:2370–81.
25. Miao HQ, Lee P, Lin H, Soker S, Klagsbrun M.

Neuropilin-1 expression by tumor cells promotes tumor angiogenesis and progression. FASEB J 2000;14:2532–9.

26. Gray MJ, Van Buren G, Dallas NA, et al. Therapeutic targeting of neuropilin-2 on colorectal carcinoma cells implanted in the murine liver. J Natl Cancer Inst 2008; 100:109–20.

27. Parikh AA, Fan F, Liu WB, et al. Neuropilin-1 in human colon cancer: expression, regulation, and role in induction of angiogenesis. Am J Pathol 2004;164: 2139–51.

28. Hansel DE, Wilentz RE, Yeo CJ, Schulick RD, Montgomery E, Maitra A. Expression of neuropilin-1 in high-grade dysplasia, invasive cancer, and metastases of the human gastrointestinal tract. Am J Surg Pathol 2004;28:347–56.

29. Caunt M, Mak J, Liang WC, et al. Blocking neuropilin-2 function inhibits tumor cell metastasis. Cancer Cell 2008;13:331–42.

30. Jung YD, Liu W, Reinmuth N, et al. Vascular endothelial growth factor is upregulated by interleukin-1β in human vascular smooth muscle cells via the p38 mitogen-activated protein kinase pathway. Angiogenesis 2001;4:155–62.

31. Arumugam T, Ramachandran V, Logsdon CD. Effect of cromolyn on S100P interactions with RAGE and pancreatic cancer growth and invasion in mouse models. J Natl Cancer Inst 2006;98: 1806–18.

32. Li JL, Harris AL. Notch signaling from tumor cells: a new mechanism of angiogenesis. Cancer cell 2005;8: 1–3.

33. Zeng Q, Li S, Chepeha DB, et al. Crosstalk between tumor and endothelial cells promotes tumor angiogenesis by MAPK activation of Notch signaling. Cancer Cell 2005;8:13–23.